

# Scanning Tunneling Microscopy and Spectroscopy Studies of Individual Lander Molecules Anchored on a Copper Oxide Nanotemplate

Y. Naitoh,<sup>†,‡</sup> F. Rosei,<sup>\*,†,§</sup> A. Gourdon,<sup>||</sup> E. Lægsgaard,<sup>†</sup> I. Stensgaard,<sup>†</sup> C. Joachim,<sup>||</sup> and F. Besenbacher<sup>\*,†</sup>

*Interdisciplinary Nanoscience Center (iNANO) and Department of Physics and Astronomy, University of Aarhus, DK-8000 Aarhus C, Denmark, Department of Applied Physics, Graduate School of Engineering, Osaka University, 2-1 Yamada-oka, Suita, Osaka 565-0871, Japan, INRS Energie, Matériaux et Télécommunications, Université du Québec, 1650 Boul. Lionel-Boulet, J3X 1S2 Varennes (QC), Canada, and Groupe Nanoscience, CEMES-CNRS, 29 Rue J. Marvig, BP 94347, 31055 Toulouse Cedex, France*

Received: June 17, 2008; Revised Manuscript Received: August 14, 2008

By means of scanning tunneling microscopy (STM), scanning tunneling spectroscopy (STS), and current image tunneling spectroscopy (CITS), we have studied the electronic properties of individual “Lander” molecules anchored on a nanopatterned Cu(110) surface. To hinder surface diffusion during STM and STS imaging and spectroscopy studies at room temperature, the molecules are immobilized in the troughs of the Cu–O nanotemplate which forms on the Cu(110) surface by exposure to oxygen at high temperature. STS spectra extracted from CITS images reveal no lateral dependency over the molecules, which indicates that the electronic features above the center of the molecules as well as above the four spacer legs are very similar. An electronic gap of  $\sim 2.2$  eV was determined from the  $dI/dV$  spectra, which is tentatively ascribed to the highest occupied molecular orbital (HOMO)–lowest unoccupied molecular orbital (LUMO) gap of the Lander molecules.

## Introduction

Custom designed organic molecules are the ultimate building blocks for the assembly of functional nanostructured materials.<sup>1–6</sup> Today, by means of organic chemistry approaches, it is indeed possible to design and synthesize molecules with well-defined functionalities, including, for example, specific mechanical and electronic properties. Using custom designed molecules such as “wires”,<sup>7</sup> “switches”,<sup>8–11</sup> and molecular diodes, transistors and small circuits can be realized.<sup>12–14</sup> Although their electronic functionalities are usually robust, when the custom synthesized molecules are adsorbed on a substrate<sup>15</sup> the molecule–surface interaction may induce changes in the molecular properties (including intramolecular structural changes) as well as local modifications in surface structure. These changes imply that the interaction between the molecules and the surface can be fairly strong in certain cases and thus significantly alter both molecular and surface properties.<sup>1,16</sup>

Within the framework of molecular electronics, a promising approach to designing monomolecular circuits is to interconnect suitable “molecular wires” to ultraclean and atomically well-defined nanoscale electrodes. A model molecular wire should be a long, linear molecule with a small highest occupied molecular orbital (HOMO)–lowest unoccupied molecular orbital (LUMO) gap and a suitable organization of molecular energy levels, so as to guide the tunneling electrons over long distances.<sup>17</sup> Several types of molecular rods with lengths up to 15 nm are available by chemical synthesis; however, most of these have a large HOMO–LUMO gap and consequently

limited electron transport properties.<sup>18</sup> The synthesis of efficient long-distance molecular wires still represents a significant challenge for organic chemistry.<sup>7,19</sup> Model prototypes of molecular wires are generally equipped with so-called lateral “spacer” groups to protect the integrity of the wire’s molecular orbitals when they are deposited on a substrate and to insulate the molecular wires from each other, thereby avoiding any cross-talk during the electrical measurements. Specifically, molecules belonging to the so-called Lander<sup>1,7</sup> family, consisting of a “conducting rod with spacer legs”, were designed and synthesized to act as molecular wires, to be used as interconnects between various nanodevices operating on an appropriate substrate. In the gas phase, the Lander molecule can adopt different minimum-energy conformations, because to some extent the spacer groups can rotate freely around the  $\sigma$ -bond, connecting them to the aromatic conducting  $\pi$ -board. The preferred molecular conformation is attained by a rotation of the spacer legs out of the right-angled orientation to the  $\pi$ -board plane, which increases the  $\pi$ – $\pi$  overlap between the aromatic core and the benzene units.

Local techniques such as scanning tunneling microscopy (STM)<sup>20,21</sup> and scanning tunneling spectroscopy (STS)<sup>22–29</sup> are ideal tools to investigate the properties of individual adsorbates with high lateral resolution (atomic or molecular), thus providing useful information on molecular functionalities (conformations, electronic properties, interaction with the substrate, etc.) after they are adsorbed on a substrate. STS measures the elastic tunneling current variation between the tip and the surface as a function of bias voltage at a specific point above the sample. The variation in the tunneling current with tunnel voltage can be used to determine the conductance ( $I/V$ ) and differential conductance ( $dI/dV$ ) of the sample and thereby the local electronic properties of the molecules. In particular, it appears that to a first approximation the normalized differential con-

\* To whom correspondence should be addressed. E-mail: rosei@emt.inrs.ca (F.R.); fbe@inano.dk (F.B.).

<sup>†</sup> University of Aarhus.

<sup>‡</sup> Osaka University.

<sup>§</sup> Université du Québec.

<sup>||</sup> Groupe Nanoscience, CEMES-CNRS.

ductance ( $dI/dV$ )/( $I/V$ ) is proportional to the local density of states of the surface. Current image tunneling spectroscopy (CITS),<sup>22,30</sup> which is obtained by acquiring STS curves at each pixel of a given image area, maintaining the tip at constant height, allows one to combine STM imaging capabilities with local spectroscopic information. A CITS image represents a tunneling current or conductance map of the surface obtained at different bias voltages, and while each image reflects the topographic corrugation of the surface, changes in contrast between images yield a two-dimensional variation of the density of electronic states on the surface.

STS data are often collected at temperatures below 15 K to reduce thermal drift, diffusion, and broadening. However, it is also important to investigate the electronic properties of organic molecules at room temperature (RT), which represents the working conditions of real devices.<sup>31</sup> Unfortunately, such investigations are particularly challenging because the relevant molecules often diffuse readily on the surface at RT<sup>32–34</sup> and thermal drift complicates the acquisition of reliable STS data. One way to circumvent the problem represented by these thermal effects is to acquire STS spectra on full molecular overlayers, because surface saturation effects prevent molecular diffusion. Another alternative approach is to form nanostructures on the surface where the molecules are anchored whereby the thermal mobility of the molecules is significantly reduced.

STM studies of the adsorption of molecules belonging to the Lander family<sup>35</sup> on Cu(001),<sup>36–38</sup> Cu(111),<sup>39,40</sup> Cu(211),<sup>41</sup> and Cu(110)<sup>16,42–46</sup> surfaces have been previously reported, and a rich variety of structures were observed due to strong molecule–surface interactions, which may induce local surface restructuring. Here, we report on STM imaging as well as STS and CITS studies at RT of individual single Lander (SL) molecules and rows of SL molecules adsorbed on oxygen induced nanopatterns on the Cu(110) surface.

## Experimental Section

The STM/STS/CITS experiments were carried out in an ultrahigh vacuum (UHV) chamber, equipped with standard techniques for surface characterization as well as the Aarhus scanning tunneling microscope,<sup>47–49</sup> operated in the 100–400 K temperature range. The Cu(110) surface was cleaned by standard sputter/annealing cycles (several cycles of Ar<sup>+</sup> ion sputtering at 2 keV followed by annealing to 823 K) to obtain pristine, atomically flat substrates.<sup>20,50</sup> The Lander molecules were loaded into a glass crucible in a home-built evaporator and thoroughly degassed at 500 K in the UHV chamber prior to use. The molecules were then adsorbed on the surface by simple sublimation from a heated glass crucible by organic molecular beam deposition (OMBD). The molecular coverage was varied by controlling the crucible temperature between 560 and 650 K (allowing variations of the deposition rate) and by changing the exposure time (60–1200 s).

To obtain the one-dimensional (1D) nanoscale grating induced by oxygen adsorption, the Cu(110) substrate was first cleaned by sputter/annealing and exposed to 3–6 langmuir (1 langmuir = 10<sup>-6</sup> Torr s) oxygen and subsequently annealed to 650 K. This procedure yields a surface template consisting of 1D bare Cu rows with a width of 2–10 nm separated by Cu–O added-row regions.<sup>51–53</sup>

The CITS images were recorded simultaneously with the STM topographic images of the molecules by acquiring the  $I-V$  characteristics at  $32 \times 32 = 1024$  points in the scanning area while stopping the scan, opening the feedback loop, and measuring the  $I-V$  curves holding the tip–surface gap instan-

## (a) Single Lander (SL) C<sub>90</sub>H<sub>98</sub>

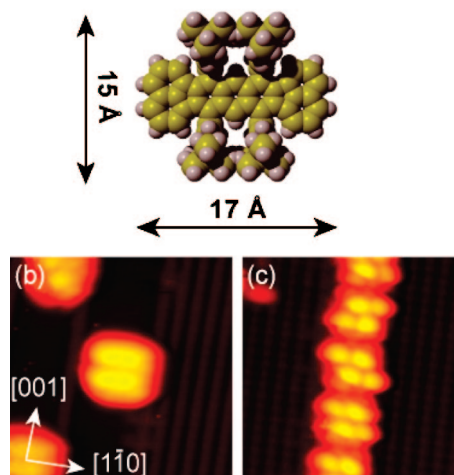


**Figure 1.** (a) Chemical structure of the Lander molecule (C<sub>90</sub>H<sub>98</sub>) consisting of a central polyaromatic board and four spacer legs. STM topographic images of rectangular and rhomboidal shaped Lander molecules adsorbed on the 1D supergrating are shown in (b) and (c), respectively (70 × 70 Å<sup>2</sup>).

taneously constant. From these measurements, we obtained information on the tunneling conductance ( $I/V$ ), and the first derivatives of the tunneling current with respect to the sample bias ( $dI/dV$ ) were calculated using home-written software. The experimental parameters used for topographic imaging were 0.2–0.3 nA for the tunnel current and –2.1 V for the sample bias. The voltage range for spectroscopy measurements was ±1.5 V.

## Results and Discussion

The prototype molecule of the Lander family investigated here, the SL (chemical composition: C<sub>98</sub>H<sub>90</sub>) molecule, is about 17 Å long and 15 Å wide and consists of a conducting board (aromatic fluoranthene  $\pi$ -system) 4.5 Å wide with four 3,5-di-*tert*-butylphenyl (DTP) “spacer legs”, with two placed on each side (cf. the structure of the molecules displayed in Figure 1a). The legs are designed so as to elevate the central  $\pi$ -system of the molecule by a nominal distance of 5 Å above the substrate upon adsorption (assuming an unperturbed conformation as in the gas phase). The actual separation of the  $\pi$ -system upon adsorption is lower, because of the attractive interaction between the central  $\pi$ -board and the surface, yet sufficient to electrically isolate the  $\pi$ -board from the surface. In this sense, the Lander board may ideally act as a molecular wire segment, even when adsorbed on a metallic support. The SL molecules on both Cu(110) and Cu(001) appear in the STM images as clusters of four bright lobes arranged in a quadrilateral geometry as revealed in Figure 1b and c. This imaging feature is also confirmed by the theoretical calculations.<sup>54,55</sup> In the STM images of the oxygen-induced reconstructed (2 × 1)O–Cu(110) surface, the characteristic Cu–O stripes running along the [001] direction are clearly visible, with atomic resolution.

Lander molecules diffuse freely on the surface at RT, which makes imaging sometimes difficult and the acquisition of spectroscopy data very challenging. It is in principle possible to acquire punctual STS spectra on individual molecules. However, during CITS acquisition, which can typically take 1 min or more, the molecule often diffuses, and the recorded CITS image becomes meaningless. Most STS studies conducted at RT report spectra obtained from full molecular coverage, which

hinders the diffusivity of the molecules. However, under such conditions, the STS spectra will be influenced by lateral interactions between the molecules.

Since our aim was to acquire spectroscopic data from individual molecules at RT, we needed to anchor single Lander molecules on the substrate to acquire stable and reproducible STS spectra and CITS images at RT. In this respect, we used the reconstructed Cu(110)-(2 × 1)O surface, which was obtained by exposing Cu(110) to oxygen at high temperature as a template surface. This procedure yields a surface template consisting of the nanoscale supergrating described above. The 1D bare Cu rows act as “surface cues”, guiding the adsorption of the SL molecules on the 1D nanoscale supergrating.<sup>56–60</sup> Figure 1b and c shows topographic images of an isolated Lander molecule with rectangular conformation and a single row of rhomboidal shaped Lander molecules, respectively, adsorbed on the bare copper rows of the O<sub>2</sub>/Cu(110)-(2 × 1)O template recorded at RT.<sup>61</sup> The Lander molecules preferentially adsorb on the bare Cu troughs, with the legs anchored at the edge of the Cu–O added row regions. As previously described,<sup>56</sup> the molecules, independently of their conformation, are oriented with their central  $\pi$ -board aligned along the [1–10] direction of the Cu(110) substrate.

Typical  $I$ – $V$  and  $dI/dV$  –  $V$  curves measured by STS are displayed in Figure 2a and b. The spectra were obtained from the center of the  $\pi$ -board and the four lobes of the Lander molecule (rectangular conformation) displayed in Figure 1b. Each of the five  $I$ – $V$  curves in Figure 2a has a flat plateau from about –0.5 to +0.7 eV, which we tentatively ascribe to its electronic gap. There is no evident spatial dependence of the spectra over the molecule; that is, the  $I$ – $V$  curves and gap do not vary significantly when acquired at different positions over the board or the lobes. The  $dI/dV$  –  $V$  curves depicted in Figure 2b show characteristic peaks at around –1.0 and +1.1 eV, which are tentatively assigned to the HOMO and the LUMO states of the Lander molecule. From this finding, we estimate the gap to be  $\sim 2.2 \pm 0.4$  eV.

The conductance ( $I/V$ ) images and the differential conductance images reproduced from  $dI/dV$  spectra are shown in the upper and lower rows, respectively, of Figure 2c. The four lobes of the molecule are clearly visible in both sets of images, indicating that the  $I/V$  and  $dI/dV$  spectra acquired in the CITS mode were not affected by any changes or deformations of the tip and/or the molecule. The CITS images ( $I/V$  and  $dI/dV$ ) can be interpreted as the integrated density of states.<sup>30</sup> The bright (yellow in our fake color scheme) contrast in the  $I/V$  images corresponds to the current channel between the tip and the sample, whereas the bright (yellow) contrast in the  $dI/dV$  images is related to the spatial distribution of the empty and filled electronic states.

Figure 3a and b displays the  $I$ – $V$  and  $dI/dV$  –  $V$  curves of a Lander molecule (rhomboidal conformation) within a molecular row on the 1D supergrating (cf. Figure 1c). Again, there is no significant variation between the five  $I/V$  spectra obtained from the center of the  $\pi$ -board and the four lobes. The  $I$ – $V$  curves are flat between –0.6 and +0.6 eV and the  $dI/dV$  –  $V$  curves have peaks at around –1.2 and +1.0 eV, from which we infer a HOMO–LUMO gap of  $\sim 2.2 \pm 0.4$  eV. The slight shift of the HOMO and LUMO peaks between the spectra of the rectangular and rhomboidal conformations may be due to a possible interaction with the adjacent molecules in the row in the case of the rhomboidal Lander molecule.

In all cases, the  $I/V$  spectra show little or no lateral dependence over the Lander molecule, that is, when acquiring

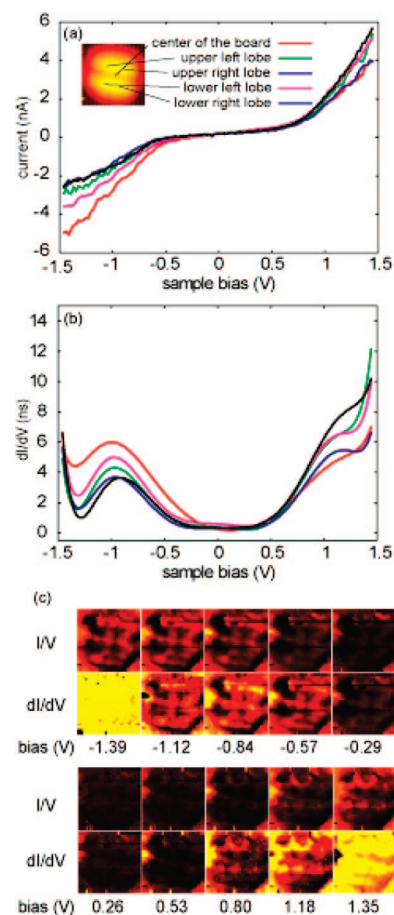


**Figure 2.** (a)  $I/V$  spectra acquired above the board’s center and the four lobes of a rectangular Lander molecule adsorbed on a bare Cu trough. (b) Differential conductance ( $dI/dV$ ) calculated from the  $I$ – $V$  curves of (a). The tunnel gap was set with the following parameters:  $I_t = 0.26$  nA,  $V_t = -2.1$  V, and  $Z_{\text{offset}} = -1.6$  Å. (c) CITS images of the Lander molecule as a function of sample bias; the upper images (set of conductance ( $I/V$ ) images) were obtained from  $I$ – $V$  spectra, while the lower images were from the  $dI/dV$  data. The color scale from black (minimum) to yellow (maximum) indicates the conductance range from 0 to 10 ns.

spectra over the central aromatic  $\pi$ -board or over the legs. Since the measured gap of  $\sim 2.2$  eV is much smaller than the high-energy gap ( $\sim 4$ – $5$  eV) expected for the DTP legs, we infer that the main contribution to the  $I/V$  spectra originates from the wave functions of the molecular wire. This implies that there is a significant leaking of the wave function of the wires over the four DTP legs. The optical gap of the SL measured in the gas phase is  $\sim 2.4$ – $2.5$  eV, which implies that the interaction with the Cu(110) surface and possibly with the adjacent Cu–O regions induces orbital mixing between the conducting board of the molecule and the substrate.<sup>62</sup>

## Conclusion

In summary, we report on STS spectra and CITS images of individual Lander molecules as well as molecular rows adsorbed on a nanopatterned Cu(110) surface at RT. To hinder surface diffusion at RT, we prepared the supergrating that forms upon exposure of the Cu(110) surface to 4–6 langmuir of oxygen at elevated temperatures. This supergrating, composed of alternating bare copper rows and (2 × 1) reconstructed Cu–O rows, acts as a template which directs the adsorption of the SL molecules.<sup>58</sup> The measured  $I/V$  and  $dI/dV$  spectra do not show any lateral dependence over the Lander molecules, as they

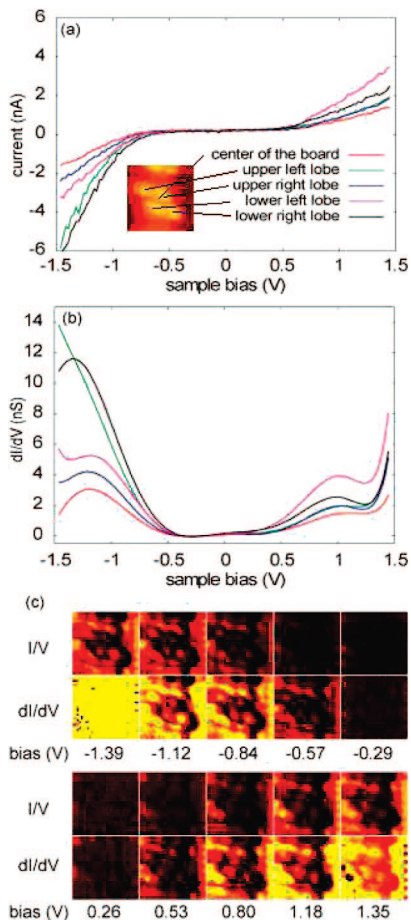


**Figure 3.** (a) Typical  $I/V$  spectra of the board center and the four lobes of a Lander molecule with *rhomboidal* conformation in a molecular row on a bare Cu trough. (b)  $dI/dV$  conformance curves extracted from the  $I-V$  curves in (a). (c) Sets of  $I-V$  and  $dI/dV$  images are provided in the upper and lower rows, respectively. The tunnel gap was set with the following parameters:  $I_t = 0.23$  nA,  $V_t = -2.1$  V, and  $Z_{\text{offset}} = -1.6$  Å. The color scale of the images depicts the conductance range from 0 to 10 nS.

exhibit very similar features above the center of the molecules as well as over the DTP spacer legs. The molecular gap measured from  $dI/dV$  curves of the spectra is found to be  $\sim 2.2 \pm 0.4$  eV, again with no spatial dependence, and is tentatively ascribed to the HOMO–LUMO gap of the molecules, possibly with some degree of coupling to the substrate. Our studies show that it is possible to exploit surface templates to position molecules and hinder their diffusion, thus permitting the acquisition of STS spectra and CITS images even at RT.

**Acknowledgment.** We acknowledge financial support from the EU through the IST Project Bottom Up Nanomachines (BUN), TMR Network AMMIST, the FUN-SMART and the PICO-INSIDE programs, as well as from the Carlsberg Foundation. We thank the Danish National Research Council for support through the Interdisciplinary Nanoscience Center (*iNANO*). F.R. acknowledges partial salary support from the EU through a Marie Curie Individual Fellowship (2001/2002), from FQRNT (Programme Strategique Nouveaux Professeurs Chercheurs, Province of Québec, 2002–2007), and from the Canada Research Chairs Program (2003 onwards). F.R. is also grateful to ISSP, University of Tokyo, for hospitality (Visiting Professorship) throughout the period November 2006 to February 2007 during which the initial draft of this manuscript was produced.

## References and Notes

- Rosei, F.; Schunack, M.; Naitoh, Y.; Jiang, P.; Gourdon, A.; Laegsgaard, E.; Stensgaard, I.; Joachim, C.; Besenbacher, F. *Prog. Surf. Sci.* **2003**, *71*, 95.
- Joachim, C.; Gimzewski, J. K.; Aviram, A. *Nature* **2000**, *408*, 41.
- Barth, J. V.; Costantini, G.; Kern, K. *Nature* **2005**, *437*, 671.
- Reed, M. A.; Tour, J. M. Computing with Molecules. *Sci. Am.* **2000**, *6*.
- Otero, R.; Rosei, F.; Besenbacher, F. *Annu. Rev. Phys. Chem.* **2006**, *57*, 497.
- Rosei, F. *J. Phys.: Condens. Matter* **2004**, *16*, S1373.
- Gourdon, A. *Eur. J. Org. Chem.* **1998**, 2797.
- Miwa, J. A.; Weigelt, S.; Gersen, H.; Besenbacher, F.; Rosei, F.; Linderoth, T. R. *J. Am. Chem. Soc.* **2006**, *128*, 3164.
- Weigelt, S.; Busse, C.; Petersen, L.; Rauls, E.; Hammer, B.; Gothelf, K. V.; Besenbacher, F.; Linderoth, T. R. *Nat. Mater.* **2006**, *5*, 112.
- Aleman, M.; Peters, M. V.; Hecht, S.; Rieder, K.-H.; Moresco, F.; Grill, L. *J. Am. Chem. Soc.* **2006**, *128*, 14446.
- Iancu, V.; Hla, S. W. *Proc. Nat. Acad. Sci. U.S.A.* **2006**, *103*, 13718.
- Perepichka, D. F.; Bryce, M. R.; Pearson, C.; Petty, M. C.; McInnes, E. J. L.; Zhao, J. P. *Angew. Chem., Int. Ed.* **2003**, *42*, 4635.
- Perepichka, D. F.; Bryce, M. R. *Angew. Chem., Int. Ed.* **2005**, *44*, 5370.
- Bendikov, M.; Wudl, F.; Perepichka, D. F. *Chem. Rev.* **2004**, *104*, 4891.
- Properties of Organic Molecules at Crystal Surfaces*; Grütter, P., Hofer, W., Rosei, F., Eds.; Imperial College Press: London, 2006.
- Rosei, F.; Schunack, M.; Jiang, P.; Gourdon, A.; Laegsgaard, E.; Stensgaard, I.; Joachim, C.; Besenbacher, F. *Science* **2002**, *296*, 328.
- Magoga, M.; Joachim, C. *Phys. Rev. B* **1998**, *57*, 1820.
- Tour, J. M. *Chem. Rev.* **1996**, *96*, 537.
- Viala, C.; Secchi, A.; Gourdon, A. *Eur. J. Org. Chem.* **2002**, 4185.
- Besenbacher, F. *Rep. Prog. Phys.* **1996**, *59*, 1737.
- Binnig, G.; Rohrer, H. *Rev. Mod. Phys.* **1999**, *71*, S324.
- Hipps, K. W. Scanning Tunneling Spectroscopy. In *Handbook of Applied Solid State Spectroscopy*; Vij, D. R., Ed.; Kluwer Scientific: New York, 2005.
- Rinaldi, R.; Cingolani, R.; Jones, K. M.; Baski, A. A.; Morkoc, H.; Di Carlo, A.; Widany, J.; Della Sala, F.; Lugli, P. *Phys. Rev. B* **2001**, *63*, 075311.
- Proehl, H.; Toerker, M.; Fritz, T.; Sellam, F.; Leo, K.; Simpson, Ch.; Müllen, K. *Phys. Rev. B* **2001**, *63*, 205409.
- Toerker, M.; Fritz, T.; Proehl, H.; Gutierrez, R.; Grosmann, F.; Schmidt, R. *Phys. Rev. B* **2002**, *65*, 245422.
- Staub, R.; Toerker, M.; Fritz, T.; Schmitz-Hübsch, T.; Sellam, F.; Leo, K. *Langmuir* **1998**, *14*, 6693.
- Voss, S.; Fonin, M.; Ruediger, U.; Burgert, M.; Groth, U. *Appl. Phys. Lett.* **2007**, *90*, 133104.
- Stipe, B. C.; Rezaei, M. A.; Ho, W. *Science* **1998**, *280*, 1732.
- Nazin, G. V.; Qiu, X. H.; Ho, W. *Science* **2003**, *302*, 77.
- Hamers, R. J. *Annu. Rev. Phys. Chem.* **1989**, *40*, 531.
- The features of spectra acquired at RT are normally broader than those of spectra acquired at LT.
- Barth, J. V. *Surf. Sci. Rep.* **2000**, *40*, 75.
- Schunack, M.; Linderoth, T. R.; Rosei, F.; Laegsgaard, E.; Stensgaard, I.; Besenbacher, F. *Phys. Rev. Lett.* **2002**, *88*, 156102.
- Weckesser, J.; Barth, J. V.; Kern, K. *J. Chem. Phys.* **1999**, *110*, 5351.
- Moresco, F.; Gourdon, A. *Proc. Nat. Acad. Sci. U.S.A.* **2005**, *102*, 8809.
- Kuntze, J.; Berndt, R.; Jiang, P.; Tang, H.; Gourdon, A.; Joachim, C. *Phys. Rev. B* **2002**, *65*, 233405.
- Zambelli, T.; Tang, H.; Lagoute, J.; Gauthier, S.; Gourdon, A.; Joachim, C. *Chem. Phys. Lett.* **2001**, *348*, 1.
- Zambelli, T.; Jiang, P.; Lagoute, J.; Grillo, S. E.; Gauthier, S.; Gourdon, A.; Joachim, C. *Phys. Rev. B* **2002**, *66*, 075410.
- Moresco, F.; Gross, L.; Aleman, M.; Rieder, K. H.; Tang, H.; Gourdon, A.; Joachim, C. *Phys. Rev. Lett.* **2003**, *91*, 036601.
- Gross, L.; Moresco, F.; Savio, L.; Gourdon, A.; Joachim, C.; Rieder, K.-H. *Phys. Rev. Lett.* **2004**, *93*, 056103.
- Aleman, M.; Gross, L.; Moresco, F.; Rieder, K.-H.; Wang, C.; Bouju, X.; Gourdon, A.; Joachim, C. *Chem. Phys. Lett.* **2005**, *402*, 180.
- Schunack, M.; Rosei, F.; Naitoh, Y.; Jiang, P.; Gourdon, A.; Laegsgaard, E.; Stensgaard, I.; Joachim, C.; Besenbacher, F. *J. Chem. Phys.* **2002**, *117*, 6259.
- Otero, R.; Rosei, F.; Naitoh, Y.; Jiang, P.; Thosttrup, P.; Gourdon, A.; Laegsgaard, E.; Stensgaard, I.; Joachim, C.; Besenbacher, F. *Nano Lett.* **2004**, *4*, 75.
- Grill, L.; Moresco, F.; Jiang, P.; Joachim, C.; Gourdon, A.; Rieder, K. H. *Phys. Rev. B* **2004**, *69*, 035416.
- Grill, L.; Rieder, K.-H.; Moresco, F.; Stojkovic, S.; Gourdon, A.; Joachim, C. *Nano Lett.* **2006**, *6*, 2685.

(46) Grill, L.; Rieder, K.-H.; Moresco, F.; Stojkovic, S.; Gourdon, A.; Joachim, C. *Nano Lett.* **2005**, *5*, 859.

(47) Lægsgaard, E.; Besenbacher, F.; Mortensen, K.; Stensgaard, I. *J. Microsc.* **1998**, *152*, 663.

(48) Lægsgaard, E.; Osterlund, L.; Thostrup, P.; Rasmussen, P. B.; Stensgaard, I.; Besenbacher, F. *Rev. Sci. Instrum.* **2001**, *72*, 3537.

(49) This instrument is now commercialized by Specs GmbH; see [http://www.specs.de/cms/front\\_content.php?idart=164](http://www.specs.de/cms/front_content.php?idart=164).

(50) Rosei, F.; Rosei, R. *Surf. Sci.* **2002**, *500*, 395.

(51) Kern, K.; Niehus, H.; Schatz, A.; Zeppenfeld, P.; George, J.; Comsa, G. *Phys. Rev. Lett.* **1991**, *67*, 855.

(52) Besenbacher, F.; Jensen, F.; Lægsgaard, E.; Mortensen, K.; Stensgaard, I. *J. Vac. Sci. Technol., B* **1991**, *9*, 874.

(53) The periodicity and width of the troughs can be fine-tuned by varying oxygen pressure and substrate temperature.

(54) Upon adsorption on a Cu surface, the spacer legs of the SL molecule can react to the tendency of the board to be attracted to the surface in different ways. On each side of the axis, because of their mutual repulsion, the two legs must move in steps, but independently of the pair on the other side. Thus, the two spacer groups on each side of the center board can each be tilted in one of two ways out of the right-angled orientation. Hence, on the surface, there are three minimum-energy conformations: two chiral (left- or right-handed) enantiomeric (mirror-image) forms with  $C2h$  symmetry (each with a crossed or staggered conformation of legs on opposite sides of the board) and one achiral form with  $C2$  symmetry (self-mirroring) (eclipsed conformation of legs on opposite sides of the board). Based on ESQC calculations,<sup>16,33,55</sup> the two different molecular shapes (rectangular and rhomboidal) found in the STM images are in turn related to the two possible geometrical conformations of the molecule on the surface. In one conformation, each pair of legs on the same side of the wire axis are parallel to each other but crossed with respect to the pair on the other side of the axis, giving an STM skewed parallelogram shape for four regions of tunneling “contact” of the spacer groups. This form is chiral, since there are two ways (“left” and “right”) to do the skewing. In the other achiral form, with the four legs all parallel to each other, only one rectangular shape for the four lobes is observed in STM images. While there is only one image form (only the “feet” of the molecule are imaged), there are two opposite ways to lean the “tops”, so when two adsorbed molecules are

adjacent along their axes, there will be a different interaction between them according to whether their “tilts” are parallel or antiparallel.

(55) We use an ESQC routine based on the calculation of the full scattering matrix of the STM tunnel junction as scans over the whole molecule. The description of this junction encompasses the surface, the adsorbate, the tip apex, and both the bulk material supporting the tip apex and the surface. Whatever the tip apex position, several hundred molecular orbitals are used to describe the electronic properties of the junction with the organic molecule positioned under the tip apex. The surface atoms and the organic molecule are described taking into account all valence molecular orbitals. Electronic interactions inside the junction are calculated using a semiempirical extended Hückel approximation with a double- $\zeta$  basis set, in order to properly reproduce the tip apex wave function in space away from the tip apex end atom. The MM2 routine used in conjunction with ESQC to optimize molecular geometries in the tunnel junction is a standard MM2 routine with a generalized potential for surface metal atoms.

(56) Otero, R.; Naitoh, Y.; Rosei, F.; Jiang, P.; Thostrup, P.; Gourdon, A.; Lægsgaard, E.; Stensgaard, I.; Joachim, C.; Besenbacher, F. *Angew. Chem., Int. Ed* **2004**, *43*, 4092.

(57) Cicoira, F.; Miwa, J. A.; Melucci, M.; Barbarella, G.; Rosei, F. *Small* **2006**, *2*, 1366.

(58) Cicoira, F.; Miwa, J. A.; Perepichka, D. F.; Rosei, F. *J. Phys. Chem. A* **2007**, *111*, 12674.

(59) Cicoira, F.; Rosei, F. *Surf. Sci.* **2006**, *600*, 1.

(60) Theobald, J. A.; Oxtoby, N. S.; Phillips, M. A.; Champness, N. R.; Beton, P. H. *Nature* **2003**, *424*, 1029.

(61) At RT on Cu(110), the molecules diffuse rapidly across the surface and are frequently found at step edges, from which we infer that the latter are sites from which diffusion is hindered. This adsorption is accompanied by the formation of Cu nanostructures protruding from the step edge, to which the molecules are effectively anchored. See refs 12 and 25–27.

(62) The measured gap was 2.3 eV for SLs adsorbed on Cu<sub>3</sub>Au(100) and 2.9 eV in the case of adsorption on Ag(111), confirming that this measurement is significantly surface dependent, as expected from the fact that SLs adopt different conformations on different substrates (Final Report of the “Bottom Up Nanomachines” EU Project, 2002).

JP8053197